Patient Specific Image Driven Evaluation of the Aggressiveness of Metastases to the Lung

Thierry Colin[1], François Cornelis[1,2], Julien Jouganous[1], Marie Martin[1], and Olivier Saut[1]

[1] Institut de Mathématiques de Bordeaux, Université de Bordeaux
[2] Hôpital Pellegrin, CHU Bordeaux

Abstract. Metastases to the lung are a therapeutic challenge because some are fast-evolving while others evolve slowly. Any insight that can be provided for which nodule has to be treated first would help clinicians. In this work, we evaluate the aggressiveness but also the response to treatment of these nodules using a calibrated mathematical model. This model is a macroscopic model describing tumoral growth through a set of nonlinear partial differential equations. It has to be calibrated to a specific patient and a specific nodule using a temporal sequence of CT scans. To this end, a new optimization technique based on a reduced order method is developed. Finally, results on two clinical cases are presented that give satisfactory numerical prognosis of the evolution of a nodule during different phases: growth, treatment and post-treatment relapse.

Keywords: Tumor growth modeling, Medical imaging, Partial Differential Equations, Clinical data assimilation.

1 Introduction

The behavior of metastases to the lung is difficult to assess by clinicians. Some may grow rapidly while some stay stationary for years. This variation makes it difficult to decide when to treat especially when elderly and weak patients are concerned. In those cases, physicians try to restrict treatment to nodules that may become malignant. A numerical tool improving the prognosis of each nodule would be invaluable in this case.

Related Works. Currently, most applications of mathematical models in clinical oncology are somehow limited to models that neglect the spatial aspect of the cancer growth like [3]. These models cannot exploit all the information provided by medical imaging devices and must be used with statistical approaches. This prevents their applications for a specific patient as they only provide "average" answers. Furthermore, these mathematical models are not able to reproduce the observed evolution of a nodule just by using two or three measurements. As this is typically the number of images available for each patient, they are not relevant here. Newer works like [1,4,9] use image data with tumor growth models. They

P. Golland et al. (Eds.): MICCAI 2014, Part I, LNCS 8673, pp. 553–560, 2014.

are mostly targeting brain tumors, are simpler from a biological point of view and the way they are calibrated on patient data uses some very specific features of the model and can not be extended to our case. We built a spatial model in order to use, in a more relevant way, the information available from anatomical imaging. Here, we are concerned with metastases to the lung of a distant tumor. The metastases are not infiltrative and diffusion-type models are not well adapted. We introduce a system of nonlinear PDEs based on populations of cells, without diffusion, but including a micro model of angiogenesis, process by which the tumor drives the emergence of its own neo-vasculature.

Once an accurate model describing tumor growth is derived, its parameters have to be recovered for any patient-specific prognosis. This complex task is usually done by solving an inverse problem using medical images [1,2]. In this work, this calibration is solved using classical approaches combining stochastic and deterministic methods. This algorithm is neither model specific, contrary to the calibration method used in [4], nor computationally expensive like solving adjoint problems [2,9].

2 Mathematical Model

The model we use in this work is derived from the one described in [5]. We consider here only one kind of cancer cells. The tumor microenvironment, and in particular the quantity of nutrients available, is essential to explain its evolution. Consequently, instead of directly modeling the nutrient density, we use a very simplified angiogenesis model to take into account the process by which the tumor escapes the avascular stage.

Cell Behavior. The tumor cell density is denoted by P and evolves by

$$\frac{\partial P}{\partial t} + \nabla \cdot (\mathbf{v}P) = (\gamma_+ - \gamma_-)P, \tag{1}$$

where $\mathbf{v}$ is the velocity corresponding to the growth of volume created by the cellular division. Coefficients for proliferation and death by hypoxia, γ_+ and γ_-, are detailed in (2) and depend on the local vascularization denoted by M. Above a given threshold of nutrient supply M_{th}, cancer cells tend to proliferate whereas, below this threshold, they starve to death. The hyperbolic tangent in both γ_+ and γ_- expressions is used to smooth and regularize the threshold functions, and K is a fixed smoothing constant. These functions are given by:

$$\gamma_{+,-}(M) = \gamma_{0,1}\frac{1 \pm \tanh(K(M - M_{th}))}{2}, \tag{2}$$

where γ_0 is the proliferation rate of non hypoxic tumor cells and γ_1 is the death by hypoxia rate. We consider that the tissue is saturated, which gives us (see [8]) an equation on $\mathbf{v}$ (3)

$$\nabla \cdot \mathbf{v} = (\gamma_+ - \gamma_-)P. \tag{3}$$

To close the system of equations (see [8]), we consider that the velocity $\mathbf{v}$ is obtained through a Darcy law in Eq.(4): $\mathbf{v}$ is derived from a pressure or potential π in the tissue.

$$\mathbf{v} = -\nabla\pi. \tag{4}$$

Angiogenesis. At the end of the avascular stage, the tumor reaches such a size that its direct environment is not able to supply enough nutrients to allow it to keep on growing. At this point, cancer cells emit chemical signals which may result in the emergence of a neo-vasculature [6]. It is described by the equations (5) and (6). The scalar variable ξ describes the total amount of pro-angiogenic agents which are produced by quiescent cells (given by the expression $\int_\Omega (1 - \frac{\gamma_+}{\gamma_0})Pd\omega$, Ω being the computing domain), and eventually metabolized.

$$\frac{\partial \xi}{\partial t} = \alpha \int_\Omega (1 - \frac{\gamma_+}{\gamma_0})Pd\omega - \lambda\xi. \tag{5}$$

As we assume that the quantity of nutrient is proportional to the density of blood vessels in the tissue, we collect these two notions in one variable M that we shall call "vasculature". The vasculature M is damaged by tumor cells and produced where the quiescent cells are located proportionally to ξ by the term $\beta\xi(1 - \frac{\gamma_+}{\gamma_0})P$.

$$\frac{\partial M}{\partial t} = -\eta PM + \beta\xi(1 - \frac{\gamma_+}{\gamma_0})P. \tag{6}$$

Taking Therapeutical Effects into Account. The model architecture makes it easy to include different types of treatment. Chemotherapy effects can be simulated adding a death term $-\delta P$ on Eq.(1) which gives:

$$\frac{\partial P}{\partial t} + \nabla \cdot (vP) = (\gamma_+ - \gamma_-)P - \delta P. \tag{7}$$

To fulfill the saturation assumption Eq.(3) is modified as follows:

$$\nabla \cdot \mathbf{v} = (\gamma_+ - \gamma_- - \delta)P. \tag{8}$$

3 Calibration Method

As shown previously, the mathematical model has many parameters, namely α, β, γ_0, γ_1, η, λ and M_{th}, that must be determined through a complex inverse problem. Most of these parameters have no physical or biological meaning and cannot be recovered by experimental measurements. Furthermore, the medical images (CT scans) have to be processed to be used with this model.

Segmentation, Registration. Lung metastases are particularly interesting from a mathematical and technical point of view because of the quality of the imagery. Indeed, in CT scans of the lung, the tumor appears as white while

healthy tissue (full of air) is mainly black. Delineating the tumor is therefore relatively easy and requires little intervention from clinicians. In practice, the segmentation is manually performed by the oncologist who choses a representative slice of the tumor. For each exam, this same slice of the tumor is segmented by the clinician. The slice is localized using physiological details such as blood vessels or bronchi. The patient is not in the same exact position for every exam. The targeted nodule is relocated to have a stationary center of gravity between scans. We made the reasonable assumption that the tumor is solid and its volume is not affected by patient's breath. The rotation of the abdomen between scans is also taken into account.

Formulation of the Inverse Problem. Given a sequence of medical images or snapshots of the tumor, we aim at finding a parameter set able to reproduce its observed behavior. Our approach is to use an objective function, which basically quantifies the difference between the observable data and the model simulation, and try to minimize it. There are different ways to measure this error and as a criterion we chose a combination of the comparison of the mass and the L^2 norm of the images. Mass is measured by integrating the cellular density P.

We need at least two images of the metastasis at different times to have a chance to personalize the model: the first one at $t_1 = 0$ is the initial condition for the tumor cell density and the other is used to parameterize the model. Whatever the minimization method, it is necessary to estimate many times the value of the objective function, and so to simulate the model for lots of parameter sets which could be quite expensive.

To make the calibration faster, we have developed a strategy based on a reduced order method called Proper Orthogonal Decomposition (POD).

Building a Reduced Order Model to Speed Up Computations. POD resolution method for dynamic systems consists in approaching partial differential equation systems with ordinary differential equations by decoupling efficiently the time and space variables (see [7]). The initial infinite dimension problem is thus replaced by a finite dimension problem.

Let us describe the POD use on the tumor cell density variable P. As we want to decouple space and time variables, we use the following representation for P (or any variable of interest): $P(X,t) = \sum_{i=1}^{d} a_i^P(t)\Phi_i^P(X) + \epsilon(X,t)$, where a_i^P are scalar functions depending on time and Φ_i^P are spatial functions called modes and represent the geometry of the variable P. The dimension of the reduced problem is denoted by d. The approximation error is denoted by $\epsilon(t,X)$. The goal of POD is to provide us with the best basis of spatial functions Φ_i^P to minimize the error.

These functions Φ_i^P are extracted from a database of admissible behaviors of P. To generate this database, we sample the parameter space using a cartesian grid, simulate the direct model for each parameter set thus obtained and keep several snapshots $(S_k^P)_k$ of the variable P. If the sample is correctly chosen, we have a representative set of geometrical configurations for the tumor cell

density. Then we look for the functions Φ_i^P in the d-dimensional vectorial space generated by the snapshots from the database. They are, in other words, linear combinations of the snapshots. These functions are taken as an orthonormal basis minimizing the truncation error of the projection which allows us to use a few modes without losing too much precision. The POD approach is used on both the tumor cell density P and the pressure field π which are the two fields driven by PDEs in our system. Finally, the system of equations is projected along these modes and so approximated by an ODE system on the coefficients $(a_i^P(t))_i$ and a linear system on the coefficients $(a_i^\pi(t))_i$.

Complete Algorithm Used for the Inverse Problem. Replacing PDEs by ODEs makes the problem simpler and faster to solve so we use this reduced model for the inverse problem. Moreover, the modes, and the spatial derivatives associated, are computed once for all. Then we use a classical optimization strategy to minimize the distance between the model simulations and the observable. The first step is to find a reasonable parameter set via a particle swarm algorithm. A sensitivity analysis was performed on the model that shows the low influence of parameters α and β. Therefore, these two parameters are fixed and a gradient algorithm is used to refine the set of parameters.

4 Results and Discussions

4.1 Trying Our Method on a First Complete Test Case

Here is a typical case of a patient with lung nodules from a primary bladder tumor.

The method described previously is used on this first test case. Six CT scans are available (the first two of which are presented in Fig.1). The first three correspond to the tumor growth. Then the nodule reached a critical volume and the clinicians decided to treat it with a chemotherapy. The two following

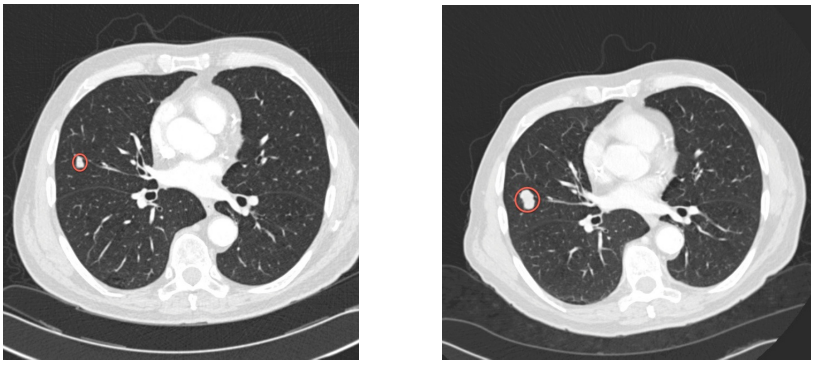

Fig. 1. Extract from a time sequence of CT scans showing the evolution of one nodule marked in red between 2008/06/07 (on the left) and 2008/09/22 (on the right)

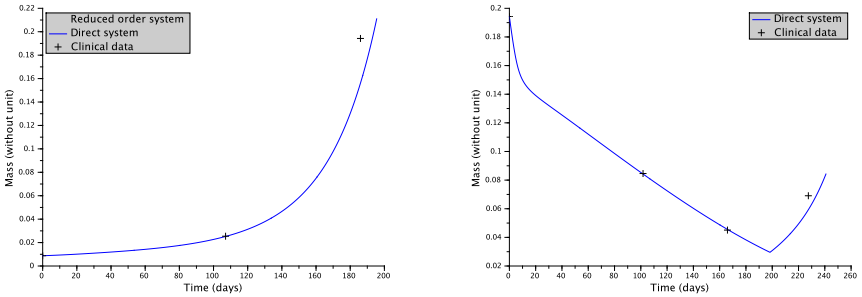

Fig. 2. Evolution of the tumoral masses as computed by our model after recovering its parameters during the growth (on the left) and after the beginning of the treatment (on the right). Tumoral masses measured on the CT scans by the clinicians are plotted with +, the reduced model simulation with dotted line and the direct model simulation with full line.

scans were used to control the response of the tumor to the treatment. Finally, a last control scan was planned after the end of the chemotherapy that showed a relapse as the tumor started growing again.

First, we use the first two scans (see Fig.1) to calibrate the model on the growth phase. Then the model is simulated up to the third scan date to see if the prediction is accurate. The tumor mass thus obtained by the model is compared to the medical data in Fig.2a.

As the model provides spatial information on the cells distribution, it is also interesting to evaluate the accuracy in shape of the results obtained with our method. For this, we used shape indicators such as the Volume Concordance (given by the expression $VC = 100 \times (1 - \frac{|P_{model} - P_{data}|}{|P_{data}|})$) and the DICE ($DICE = 100 \times (\frac{2*|P_{model} \bigcap P_{data}|}{|P_{model}|+|P_{data}|})$). We also compute a reference DICE between the first scan which is the initial condition of our system and the current scan. This represents the hypothesis of a non evolving tumor and gives a value of comparison. Moreover, the temporal prediction error is another significant indicator. If we denote by t_i the time of the i^{th} exam and t'_i the time when the simulated tumor reaches the size of the real tumor at the i^{th} exam; it is relevant to look at the delay between the simulation and the real case $t_i - t'_i$ and the normalized delay $100 \times \frac{t_i - t'_i}{t_i - t_0}$, $i = 1, 2$. These four indicators are given on Table 1.

Then, we tried to calibrate the treatment parameter δ to see if the response to the chemotherapy is predictable with our tool. Here only one parameter has to be determined which makes this second inverse problem easier than the first one. The initial condition we used for P is the last scan before treatment on 2008/12/10 and we used the first control scan during chemotherapy to calibrate the treatment parameter. The evolution of the tumor mass during the treatment provides a good insight into the therapeutical efficacy. It is given in Fig.2b and we can see that here again the model is predictive for this case and provides a

Table 1. Scalar indicators for the tumor growth of the first clinical case: DICE, Volume Concordance and delays

Date	2008/09/22	2008/12/10
DICE	90.96%	87.21%
reference DICE	54.94%	10.25%
Volume Concordance	82.54%	77.76%
Delay (days)	0	-6.7
Normalized Delay	0%	-3.6%

Table 2. Scalar indicators for the tumor under chemotherapy and rebound of the first clinical case: DICE, Volume Concordance and delays

Date	2009/03/21	2009/05/27	2009/07/27
DICE	92.26%	87.44%	84.79
reference DICE	57.63%	37.71%	52.78
Volume Concordance	84.4%	74.56%	69.9
Delay (days)	0.3	0.6	-6.4
Normalized Delay	0.1 %	0.2 %	-2.8%

Table 3. Scalar indicators for the tumor growth of the second test case: DICE, Volume Concordance and delays

Date	2010/03/11	2010/07/16
DICE	85.41%	88.69%
reference DICE	65.93%	38.09%
Volume Concordance	70.59%	76.45%
Delay (days)	0	5.6
Normalized Delay	0%	2.3%

good estimation of the response of the patient to this chemotherapy. Moreover, after the end of the treatment, the tumor started growing again and this relapse is also well predicted by the model. The same indicators that were used for the growth are given in Table 2. For the last exam, on 2009/07/27, the shape indicators are not relevant as the relapse is located at the periphery of the initial nodule and so the shape and location can not be predicted accurately.

4.2 A Second Test Case

The whole calibration method described previously is used on another case of tumoral growth. Here again, we use two scans at different time points to calibrate the model and a third image to quantify the accuracy of the prediction. The indicators are given in Table 3.

In this case, the growth is slower than in the previous one and the model is able to reproduce such a kind of dynamics. Indeed, the time error in prediction is about 6.4 days which, at the time scale we used and considering the tumor registration uncertainties, is a good result.

In each case, we always considered the same slice of the tumor. The same technique can be applied on the whole 3D volume reconstructed from the medical images which would enable us not to choose a particular slice. The complete method thus developed was successful to provide us with a relevant prognosis on the evolution of lung nodules for several clinical cases. A larger study on about 20 patients is ongoing to evaluate the quality of the prognosis on a larger scale.

References

1. Clatz, O., Sermesant, M., Bondiau, P.-Y., Delingette, H., Warfield, S.K., Malandain, G., Ayache, N.: Realistic simulation of the 3-d growth of brain tumors in mr images coupling diffusion with biomechanical deformation. IEEE Transactions on Medical Imaging 24(10), 1334–1346 (2005)
2. Hogea, C., Davatzikos, C., Biros, G.: An image-driven parameter estimation problem for a reaction–diffusion glioma growth model with mass effects. J. Math. Biol. 56(6), 793–825 (2008)
3. Simeoni, M., Magni, P., Cammia, C., Nicolao, G.D., Croci, V., Pesenti, E., Germani, M., Poggesi, I., Rocchetti, M.: Predictive pharmacokinetic-pharmacodynamic modeling of tumor growth kinetics in xenograft models after administration of anticancer agents. Cancer Res 64(3), 1094–1101 (2004)
4. Swanson, K.R., Alvord, E.C., Murray, J.D.: Virtual brain tumours (gliomas) enhance the reality of medical imaging and highlight inadequacies of current therapy. Br. J. Cancer 86(1), 14–18 (2002)
5. Colin, T., Iollo, A., Lombardi, D., Saut, O.: System identification in tumor growth modeling using semi-empirical eigenfunctions. Mathematical Models and Methods in Applied Sciences (2012)
6. Carmeliet, P., Jain, R.: Angiogenesis in cancer and other diseases. Nature (2000)
7. Kunisch, K., Volkwein, S.: Galerkin proper orthogonal decomposition methods for parabolic problems. Numer. Math, 117–148 (2001)
8. Ambrosi, D., Preziosi, L.: On the closure of mass balance models for tumor growth. Math. Mod. Meth. Appl. Sci 12(5), 737–754 (2002)
9. Liu, Y., Sadowski, S.M., Weisbrod, A.B., Kebebew, E., Summers, R.M., Yao, J.: Patient Specific Tumor Growth Prediction Using Multimodal Images. Medical Image Analysis (2014)